Synthesis and Properties of Mesogen-Jacketed Liquid Crystalline Polymers Containing Biphenyl Mesogen with Asymmetric Substitutions

LANYING ZHANG, HONGLIANG WU, ZHIHAO SHEN, XINGHE FAN, QIFENG ZHOU

Beijing National Laboratory for Molecular Sciences, Key Laboratory of Polymer Chemistry and Physics of Ministry of Education, College of Chemistry and Molecular Engineering, Peking University, Beijing 100871, China

Received 1 February 2011; accepted 26 April 2011
DOI: 10.1002/pola.24757

ABSTRACT: This work focuses on the design, synthesis, and characterization of a series of mesogen-jacketed liquid crystalline polymers (MJLCPs), poly(alkyl 4′-(octyloxy)-2-vinylbiphenyl-4-carboxylate) (pVBP(m,8), m = 1, 2, 4, 6, 8, 10, 12). For the first time, we realized asymmetric substitutions in the mesogens of MJLCPs. The polymers obtained by conventional free radical polymerization were investigated in detail by a combination of various techniques, such as differential scanning calorimetry, wide-angle X-ray diffraction, and polarized light microscopy. Our results showed that all the polymers were thermally stable, and their glass transition temperatures decreased when m increased. The liquid crystalline (LC) phases that developed at high temperatures and disappeared at low temperatures were strongly dependent on the difference in lengths of alkyl groups on the 4 and 4′ substitution positions of the side-chain biphenyl. While polymer pVBP(1,8) was not liquid crystalline, columnar liquid crystalline phases were observed for all other pVBP(m,8) (m = 2, 4, 6, 8, 10, 12) polymers. Polymer pVBP(8,8) showed a tetragonal columnar nematic liquid crystalline phase, and the other LC polymers exhibited columnar nematic phases. In additions, the smaller the difference in the lengths of the terminal alkyls, the easier the development of the liquid crystalline phase. Birefringence measurements showed that solution-cast polymer films exhibited moderately high positive birefringence values, indicating potential applications as optical compensation films for liquid crystal displays. © 2011 Wiley Periodicals, Inc. J Polym Sci Part A: Polym Chem 49: 3207–3217, 2011

KEYWORDS: liquid-crystalline polymers (LCP); phase behavior; supramolecular structures

INTRODUCTION The design and synthesis of soft matter is a hot topic of research and is very important for functional materials science and life science. Liquid crystalline polymers (LCPs), especially side-chain liquid crystalline polymers (SCLCPs), which combine the ordered structures of liquid crystals and the excellent properties of polymers, have attracted considerable attention and become one of the most important research fields in polymer chemistry and physics due to their outstanding applications in engineering plastics, optic and electro-optic devices, and so on.[1] For SCLCPs, the mesogens can be either terminally or laterally attached to the polymer backbone. According to Finkelmann's principle, flexible spacers are needed to decouple motions of the main chain and the mesogenic side groups.[2] However, as proposed by Zhou, mesogen-jacketed liquid crystalline polymers (MJLCPs), which are a special class of SCLCPs with their mesogenic units attached laterally to the main chain through a short spacer[3] or only one covalent C—C bond,[4] can also form stable liquid crystalline phases. The bulky and rigid mesogenic units directly linking to the polymer backbone force the main chain to take an extended chain conformation. MJLCPs exhibit properties similar to those of main-chain LCPs (MCLCPs), such as large persistence length in good solvents[5] and banded texture of the sheared liquid crystalline (LC) phase.[6] One-dimensional (1D) and two-dimensional (2D) wide-angle X-ray diffraction (WAXD) investigations combined with polarized light microscopy (PLM) and differential scanning calorimetry (DSC) results have revealed that one of the most common phase structures of MJLCPs is the columnar nematic (Φ_N) phase.[7] Higher-ordered LC phases, such as hexagonal columnar (Φ_H) phase,[8] hexatic columnar nematic (Φ_{HN}) phase,[9] and smectic A[10] or smectic C[11] phase, have also been observed in some systems.

Since the first publication on MJLCPs, up to date, a rich variety of MJLCPs with different structures and unique properties have been rationally designed and synthesized. Among them, there are three series of MJLCPs (Chart 1), which are based on 2-vinylterephthalic acid with alkyl[8] or aryl ester,[7] 2-vinyl-terphenyl with alkyl ester[12] or alkyl ether,[13] and 2(or 3)-vinylbiphenyl-4,4′-dicarboxylic acid with aryl.[11] Poly[di(alkyl) vinylterephthalates] with suitable tail lengths[8] can form stable long-range-ordered Φ_H phases, and the polymers

Additional Supporting Information may be found in the online version of this article. Correspondence to: Z. Shen (E-mail: zshen@pku.edu.cn) or X. Fan (E-mail: fanxh@pku.edu.cn)

Journal of Polymer Science Part A: Polymer Chemistry, Vol. 49, 3207–3217 (2011) © 2011 Wiley Periodicals, Inc.

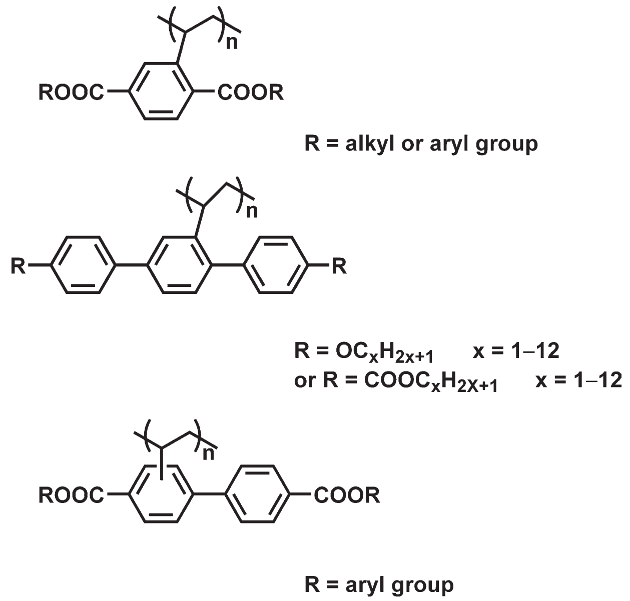

CHART 1 Chemical structures of the three series of mesogen-jacketed liquid crystalline polymers.

based on 5-terphenyl, poly[2,5-bis(4′-alkoxycarbonylphenyl)-styrene]s, with longer alkoxy tails ($m = 3-12$)[13] exhibit Φ_N phases at high temperatures. On the other hand, whether polymers based on the biphenyl mesogenic core can still self-assemble into stable LC phases is a subject that has not been fully investigated, although biphenyl itself as a mesogenic group has long been widely used as the liquid crystalline core of small molecules[14–16] or building blocks in main-chain,[17] side-chain,[18–23] and main-chain/side-chain[24] LCPs. Percec et al.[25] synthesized jacketed LCPs, poly(*p*-phenylene)s (PPPs) containing 4-cyano-4′-biphenylyl mesogenic side groups with spacers of different lengths, and found the first examples of the N_{II} phase. They also designed and synthesized a series of self-organized helical dendronized, therefore, also jacketed, polyphenylacetylenes (PPAs) exhibiting a hexagonal columnar lattice with an internal order and a hexagonal columnar liquid crystalline phase.[26,27] Furthermore, the alkyl tails are all the same for the MJLCPs synthesized previously, with more attention paid to the effect of the tail length, but the influence of the relative length of the terminal alkyl groups on the phase structures has not been studied. Although Thayumanavan and coworkers have recently reported the self-assembling behaviors in solution of some polystyrene-based amphiphilic homopolymers containing two benzene rings connected by methoxy in the side chain, their bulk liquid crystalline properties have not been examined.[28,29]

Liquid crystal displays (LCDs) play important roles in our modern life. Polymers have been utilized as optical compensators for improved viewing angles in LCDs, owing to their unique optical properties,[30] easy processing, and low cost for device integration, and high birefringence, either positive or negative, of the polymeric flexible thin film is preferred. Obtaining polymer films with highly positive birefringence is challenging. At present, commercial polymeric optical compensators with positive birefringence require expensive post-processing such as rubbing,[31] stretching,[32] light irradiation,[33] or application of a high electric field,[34] all of which will unavoidably increase the cost. We have recently reported solution-cast MJLCP films with strikingly high positive birefringence values of up to 0.0350 without any postprocessing, which hold tremendous promise for application in optical compensators.[35] However, their usually poor film-forming ability and high cost in synthesis limit widespread applications of these polymers.

Herein, we present the first example of MJLCPs based on biphenyl mesogenic cores with asymmetric substitutions of alkyl tails with different lengths. A series of poly(alkyl 4′-(octyloxy)-2-vinylbiphenyl-4-carboxylate) (pVBP(m,8), m = 1, 2, 4, 6, 8, 10, 12) were successfully synthesized by conventional free radical polymerization in solution. The resultant polymers are therefore a model system to investigate the effect of the difference in lengths of the two terminal alkyl groups on the LC phase structure and phase transition.

EXPERIMENTAL

Materials

Methyl 4-bromo-3-methylbenzoate (98%, Alfa Aesar), 4-(octyloxy)phenylboronic acid (99.6%, Alfa Aesar), triphenylphosphine (99%, Alfa Aesar), 40% formaldehyde (AR, Beijing Yi Li Chemical), *N,N*′-dicyclohexyl carbodiimide (DCC, 95%, Sinopharm Chemical Reagent), 4-dimethylaminopyridine (DMAP, 99%, ACRO), and *N*-bromosuccinimide (NBS, 99%, Aldrich) were used as received without further purification. Azobisisobutyronitrile (AIBN) was recrystallized from ethanol before use. Benzoyl peroxide (BPO) was recrystallized from chloroform and methanol. Chlorobenzene was washed with H_2SO_4, $NaHCO_3$, and distilled water and then distilled from calcium hydride. Tetrahydrofuran (THF, AR, Beijing Chemical) was refluxed over sodium and distilled before use. Dichloromethane (AR, Beijing Chemical) was dried over magnesium sulfate anhydrous.

Monomer Synthesis

The synthetic route of monomers is represented in Scheme 1. The experimental details are described as follows.

Synthesis of 4-Bromo-2-Vinylbenzoic Acid

Methyl 4-bromo-3-methylbenzoate (8.030 g, 0.035 mol), NBS (9.362 g, 0.053 mol), and BPO (0.1697 g, 0.701 mmol) were dissolved in 160 mL of CCl_4 and refluxed for 6 h. The floating succinimide was filtered off, and the solvent was evaporated. Then the residue was boiled with 9.197 g (0.035 mol) of triphenylphosphine in 180 mL of acetone for 6 h until white phosphonium salt precipitated. NaOH aqueous solution (5 M, 250 mL) was added slowly to 190 mL of 40% formaldehyde containing 9.715 g (0.017 mol) of the above phosphonium salt obtained, and the mixture was stirred for 48 h at ambient temperature. After the floating substance was filtrated off, the resultant crude product was washed by 5 M NaOH aqueous solution twice. HCl (12 M) was added to the filtrate until the pH of the solution was less than 1, and then

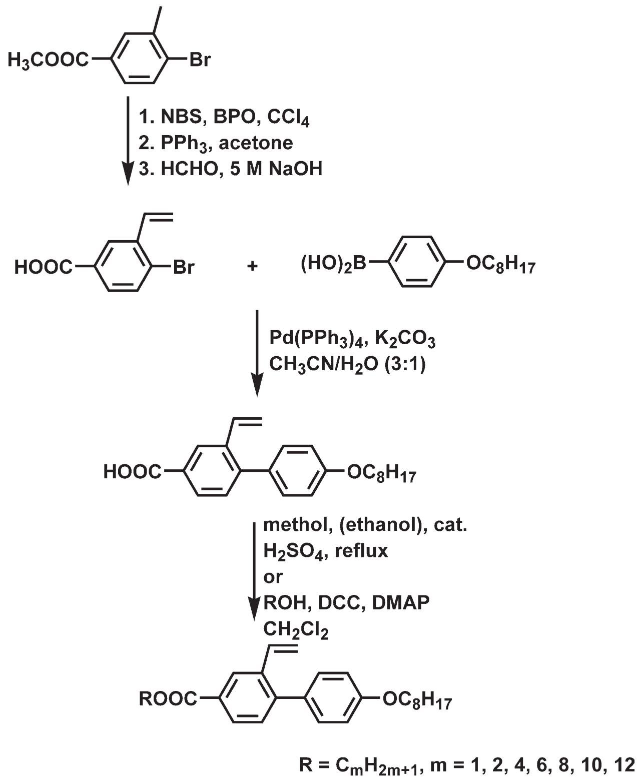

SCHEME 1 Synthetic route of styrene liquid crystalline monomers.

white product appeared. Yield: 60%. ^{1}H NMR (δ, ppm, DMSO$-d_6$): 5.508–5.536 (d, 1H, $=$CH*H*), 5.901–5.944 (d, 1H, $=$C*H*H), 6.961–7.032 (q, 1H, CH$=$), 7.738–7.787 (m, 2H, Ar), 8.153–8.156 (d, 1H, Ar). MS: 226 (m/e).

Synthesis of Pd(PPh$_3$)$_4$

Pd(PPh$_3$)$_4$ was prepared according to the method reported in literature.[36]

Synthesis of 4′-(Octyloxy)-2-Vinylbiphenyl-4-Carboxylic Acid (mVBP(0,8))

In this step, a typical Suzuki cross-coupling reaction was used. 4-Bromo-2-vinylbenzoic acid (7.762 g, 0.034 mol), 4-(octyloxy)phenylboronic acid (9.240 g, 0.037 mol), Pd(PPh$_3$)$_4$ (0.126 g, 1.109 mol), and potassium carbonate (K$_2$CO$_3$, 9.274 g, 0.067 mol) were mixed in a 250-mL three-necked flask under an argon atmosphere. Then 160 mL of acetonitrile/water (3/1) mixture was added and refluxed at 80 °C for 40 h. The mixture was cooled to ambient temperature and filtrated to remove the floating substance. HCl (50 mL, 12 M) was added to the filtrate, and then a white solid appeared. The mixture was filtered, and the obtained white solid was washed with acetonitrile twice. Yield: 80%.

^{1}H NMR (δ, ppm, DMSO$-d_6$): 0.837–0.871 (t, 3H, terminal CH$_3$), 1.257–1.307, 1.393–1.413, 1.699–1.736 (m, 12H, (CH$_2$)$_6$), 3.976–4.009 (t, 2H, OCH$_2$), 5.282–5.311, 5.791–5.835 (d, 2H, $=$CH$_2$), 6.627–6.671 (q, 1H, CH$=$), 6.999–7.020 (d, 2H, Ar), 7.244–7.265 (d, 2H, Ar), 7.367–7.387 (d, 1H, Ar), 7.873–7.897 (m, 1H, Ar), 8.181–8.184 (d, 1H, Ar), 13.048 (s, 1H, COOH). MS: 352 (m/e).

Synthesis of Methyl 4′-(Octyloxy)-2-Vinylbiphenyl-4-Carboxylate (mVBP(1,8))

4′-(Octyloxy)-2-vinylbiphenyl-4-carboxylic acid (1 g, 2.841 mmol) in 60 mL of methanol with 5 drops of sulfuric acid (98%) was refluxed for 24 h. After methanol was evaporated under reduced pressure, the crude product was dissolved in CH$_2$Cl$_2$ and extracted with saturated solution of NaHCO$_3$. The combined organic layer was dried by magnesium sulfate anhydrous. Then the product was obtained after the solvent was removed. Yield: 98%. ^{1}H NMR (δ, ppm, CDCl$_3$): 0.875–0.909 (t, 3H, terminal CH$_3$), 1.254–1.376, 1.454–1.492, 1.768–1.821 (m, 12H, CH$_2$), 3.935 (s, 3H, COOCH$_3$), 3.970–4.003 (t, 2H, OCH$_2$), 5.240–5.268, 5.772–5.816 (d, 2H, $=$CH$_2$), 6.696–6.767 (q, 1H, CH$=$), 6.931–6.960 (m, 2H, Ar), 7.245–7.273 (m, 2H, Ar), 7.320–7.340 (m, 1H, Ar), 7.930–7.954 (m, 1H, Ar), 8.287–8.291 (d, 1H, Ar). ^{13}C NMR (δ, ppm, CDCl$_3$): 167.047, 158.814, 144.863, 136.001, 135.384, 131.870, 130.732, 130.192, 128.752, 128.433, 127.318, 115.638, 114.135, 68.059, 52.123, 31.807, 29.355, 29.266, 29.236, 26.059, 22.650, 14.092. MS: 366 (m/e).

Synthesis of Butyl 4′-(Octyloxy)-2-Vinylbiphenyl-4-Carboxylate (mVBP(4,8))

4′-(Octyloxy)-2-vinylbiphenyl-4-carboxylic acid (0.500 g, 0.001 mol), *n*-butanol (0.526 g, 0.007 mol), DCC (0.293 g, 0.001 mol), and DMAP (0.052 g, 0.426 mmol) were dissolved in dichloromethane. The solution was stirred at ambient temperature for about 24 h. The precipitate was filtered and washed with dichloromethane for several times. After evaporation of the solvent, the ester obtained was purified by silica gel column chromatography with dichloromethane as the eluent to yield 0.208 g (51%) of the product.

^{1}H NMR (δ, ppm, CDCl$_3$): 0.878–0.911 (t, 3H, terminal CH$_3$), 0.978–1.015 (t, 3H, terminal CH$_3$), 1.298–1.356, 1.398–1.478, 1.789–1.826 (m, 16H, CH$_2$), 3.984–4.017 (t, 2H, OCH$_2$), 4.341–4.374 (t, 2H, COOCH$_2$), 5.247–5.276, 5.775–5.819 (d, 2H, $=$CH$_2$), 6.701–6.773 (q, 1H, CH$=$), 6.941–6.963 (m, 2H, Ar), 7.255–7.282 (m, 2H, Ar), 7.328–7.348 (m, 1H, Ar), 7.940–7.964 (m, 1H, Ar), 8.288–8.291 (d, 1H, Ar). ^{13}C NMR (δ, ppm, CDCl$_3$): 166.507, 158.743, 144.689, 135.885, 135.367, 131.832, 130.663, 130.072, 129.074, 128.338, 127.210, 115.502, 114.053, 67.095, 64.775, 31.762, 30.751, 29.312, 29.219, 29.197, 26.017, 22.605, 19.227, 14.043, 13.720. MS: 408 (m/e).

Syntheses of other monomers can be found in the Supporting Information.

Polymer Synthesis

All polymers were obtained via conventional free radical polymerization in solution, as shown in Scheme 2. A typical polymerization procedure is summarized as the following. About 0.538 g of mVBP(6,8), 15 μL of 0.106 M AIBN/chlorobenzene solution, and 1.244 g of chlorobenzene were transferred into a polymerization tube. After three freeze-pump-thaw cycles, the tube was sealed under vacuum.

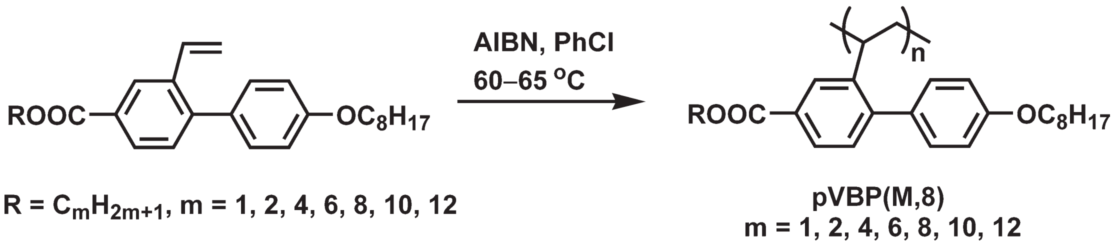

SCHEME 2 Chemical structures and synthesis of the polymers.

Polymerization was carried out in an oil bath at 60–65 °C for 48 h. It was stopped by dipping the tube in ice/water, and the tube was broken. The mixture was diluted with about 10 mL of THF and precipitated into methanol twice to yield a white product. After purification, the polymer was dried under vacuum for 2 d.

Characterization

^{1}H NMR spectra, mass spectra (MS), gel permeation chromatographic (GPC) measurements, thermogravimetric analyses (TGA), DSC, PLM, and WAXD (1D and 2D) experiments were performed according to the procedures described previously,[37] except that 2D WAXD patterns at various temperatures were recorded utilizing a hot stage set up on the diffractometer with a temperature accuracy of ±1 °C. Birefringence (Δn) values of the monomers were estimated by the host-guest method in literature.[38] Birefringence values of the free-standing polymer films were measured by a prism coupler (Model 2010, from Metricon) at 633 nm.[39] Sample preparation followed the procedures in the literature.[35]

RESULTS AND DISCUSSION

Synthesis and Characterization of the Monomers and Polymers

As shown in Scheme 1, the monomers could be successfully synthesized through a multistep reaction route. The structures of the monomers and precursors were confirmed by ^{1}H NMR, ^{13}C NMR, and mass spectrometry.

Figure 1 presents the ^{1}H (part a) and ^{13}C (part b) NMR spectra ($CDCl_3$–*d*) of the monomer mVBP(1,8) and the ^{1}H NMR spectrum (part c) of the corresponding polymer pVBP(1,8). The spectrum of mVBP(1,8) showed the representative resonances of the vinyl group at 5.24–5.82 and 6.70–6.77 ppm. After polymerization, these signals completely disappeared. The resonance peaks of the spectrum of pVBP(1,8) were broad due to the slower motion of the protons, which was common for polymers. All other monomers and polymers were characterized similarly, and the results were in accordance with the desired structures. The polymers were completely soluble in common organic solvents, such as dichloromethane, chloroform, acetone, THF, chlorobenzene, and so on.

The preliminary characterization results of the polymers are summarized in Table 1. GPC analysis was performed to determine the apparent molecular weights (MWs) and molecular weight distributions of the polymers. The typical GPC traces of all the polymers are shown in Supporting Information (Fig. S1). The apparent number average molecular

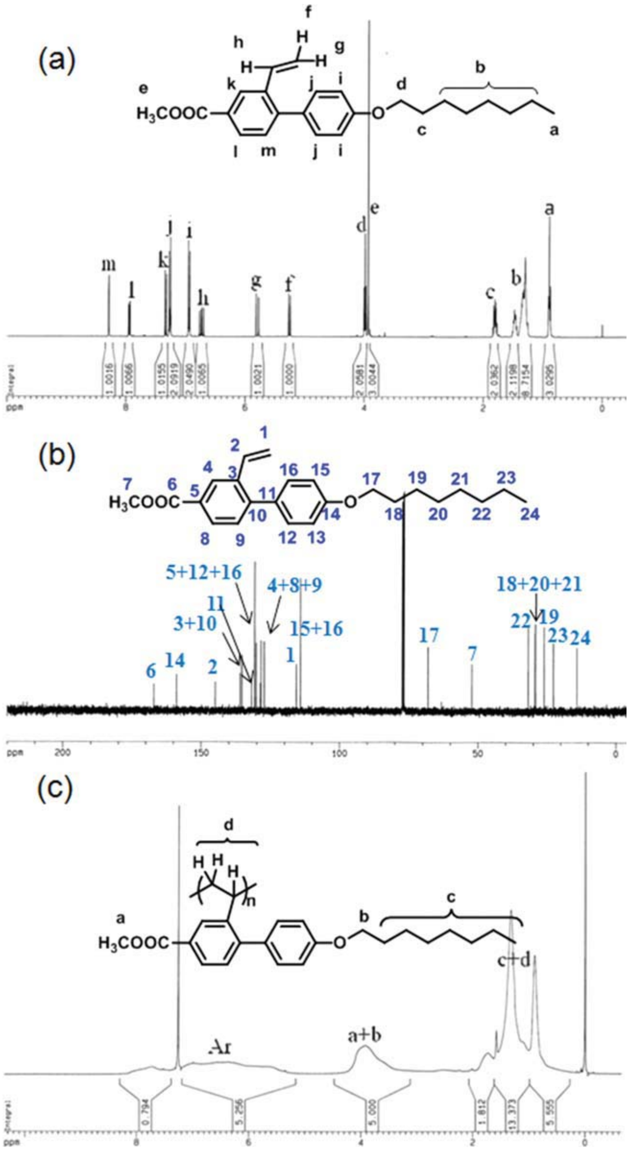

FIGURE 1 ^{1}H (a) and ^{13}C (b) NMR spectra of methyl 4′-(octyloxy)-2-vinylbiphenyl-4-carboxylate, mVBP(1,8) and ^{1}H NMR spectrum of poly{methyl 4′-(octyloxy)-2-vinylbiphenyl-4-carboxylate}, pVBP(1,8) (c). [Color figure can be viewed in the online issue, which is available at wileyonlinelibrary.com.]

TABLE 1 Molecular Weights, Polydispersity Indexes, 5% Weight Loss Temperatures, Glass Transition Temperatures, and Liquid Crystallinity of the Polymers

Sample	M_n ($\times 10^4$ g/mol)[a]	PDI[a]	T_d (°C)[b]	T_g (°C)[c]	Liquid Crystallinity[d]
pVBP(1,8)	10.8	1.34	392	126	No
pVBP(2,8)	12.0	1.31	381	95	Yes
pVBP(4,8)	15.1	1.16	385	76	Yes
pVBP(6,8)	10.5	1.37	396	64	Yes
pVBP(8,8)	9.2	1.46	369	57	Yes
pVBP(10,8)	11.8	1.27	369	44	Yes
pVBP(12,8)	10.4	1.38	392	42	Yes

[a] The apparent M_n and PDI values were measured by GPC using PS standards.
[b] The temperatures at 5% weight loss of the samples under nitrogen were measured by TGA heating experiments at a rate of 20 °C/min.
[c] The glass transition temperatures of the samples under a nitrogen atmosphere were measured by DSC at a scanning rate of 10 °C/min.
[d] Determined by the combination of PLM and 1D WAXD observations.

weights (M_n's) of all the polymers were about 10 × 10^4 g/mol and polydispersity indexes (PDIs) were below 1.50, which showed good polymerizability of the monomers. All polymers were quite thermally stable under the nitrogen atmosphere and their 5% weight loss temperatures (T_d's) were above 368 °C as shown in Table 1.

Phase Transitions and Phase Structures of the Monomers and Polymers

All the monomers were light yellow liquid at ambient temperature, and no mesophases were detected in PLM experiments at higher temperatures.

The phase transitions of the polymers were first examined by DSC experiments. To eliminate the complex thermal history of the samples generated during solvent evaporation and drying, the second DSC heating traces were used to determine the T_g values. All the DSC curves showed only glass transitions (listed in Table 1), and no other transition processes were observed, as found for most other MJLCPs reported previously.[7,11] The T_g's of the polymers gradually decreased with increasing m due to enhanced internal plasticization. Because the DSC method was not sensitive enough to determine the phase transitions of these polymers except for glass transitions, PLM and WAXD techniques were utilized.

Birefringence of the polymers was observed under PLM with the films cast from $CHCl_3$ solutions and slowly dried at ambient temperature. At ambient temperature, all the polymers exhibited only very weak birefringence, presumably due to the existence of certain alignment of the polymer chains during precipitation. Upon heating, the polymers behaved differently depending on the length of the alkyl ester. Polymer pVBP(1,8), which had the shortest alkyl ester tails, displayed no discernible change even when heated up to 250 °C. For polymer pVBP(2,8), obvious birefringence could be observed when the sample was heated to a temperature higher than T_g. A typical texture, which was schlieren-like, developed during further heating is shown in Figure 2(a). However, when m was more than 2 (i.e., m = 4, 6, 8, 10, 12), distinct texture [as shown in Fig. 2(b), taking pVBP(8,8) as an example] that was quite different from that of pVBP(2,8) could be observed when the temperature was much higher than T_g. When shearing was applied to these samples in their LC states, a banded texture formed, with the shear direction parallel to the normal of the bands [Fig. 2(c), taking pVBP(10,8) as an example]. The banded texture is usually regarded as the characteristic texture for rod-like molecules, such as main-chain liquid-crystalline polymers.[40] In addition, the banded texture remained unchanged upon the isothermal process. This confirmed again that structurally side-chain-type MJLCPs displayed some properties represented by rigid or semirigid MCLCPs.[6]

The phase transitions of the polymers were further verified by variable-temperature, 1D WAXD experiments. Sets of 1D WAXD profiles of the as-cast sample of pVBP(1,8) recorded during the first heating and subsequent cooling processes are presented in Figure 3. The as-cast amorphous sample demonstrated two scattering halos in a low-angle region of 2–7.5° and a high-angle region of 15–25° at low temperatures. The scattering halo in the low-angle region increased

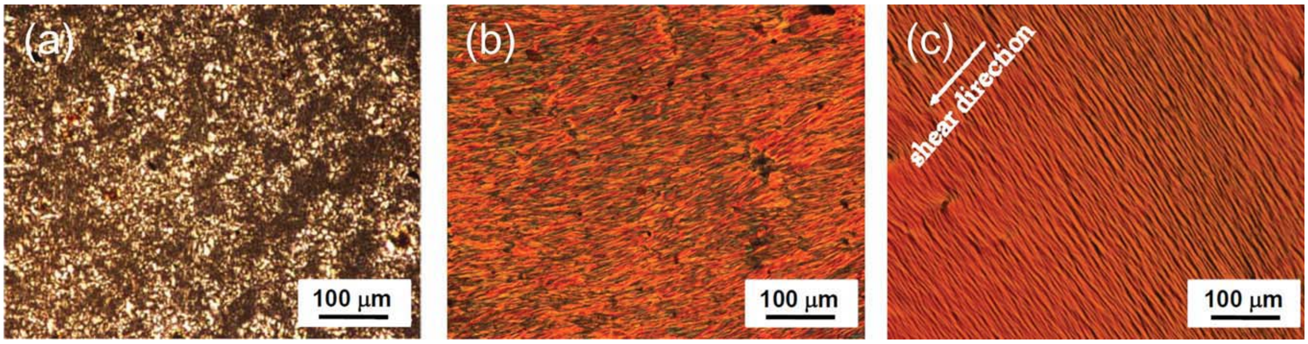

FIGURE 2 Polarized light microscope images of solution-cast films of pVBP(2,8) taken at 230 °C (a), pVBP(8,8) taken at 210 °C (b), and mechanically sheared solution-cast film of pVBP(10,8) taken at 250 °C (c).

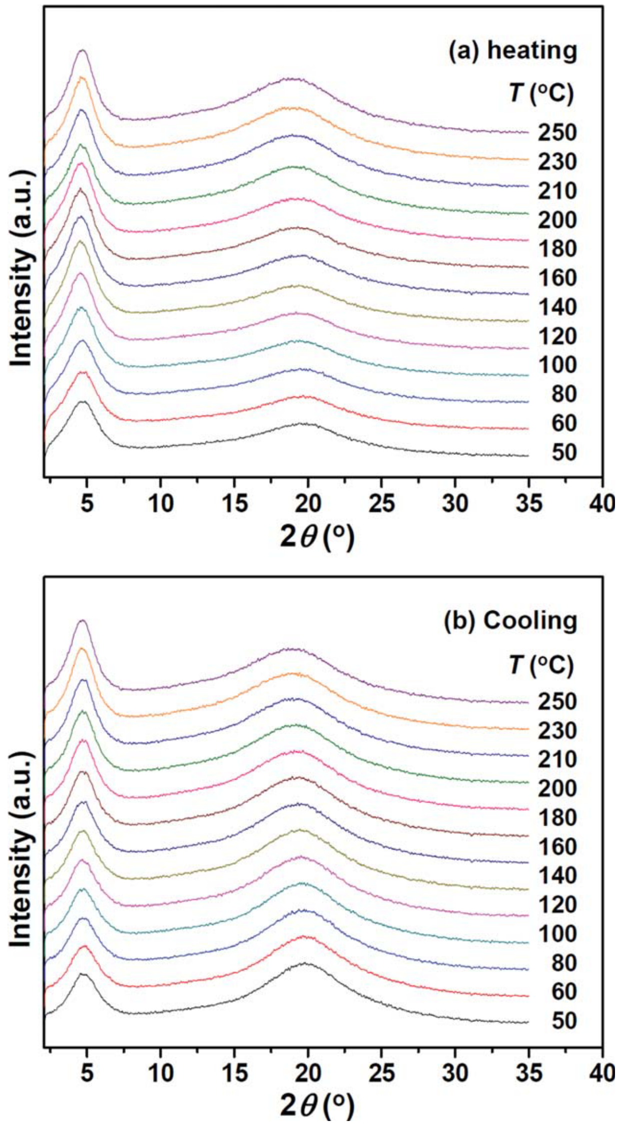

FIGURE 3 1D WAXD powder patterns of pVBP(1,8) during heating (a) and cooling (b) processes under a nitrogen atmosphere. [Color figure can be viewed in the online issue, which is available at wileyonlinelibrary.com.]

in intensity with increasing temperature, but remained as a broad scattering for the entire temperature region. Combining with the PLM results, we concluded that this polymer was not liquid crystalline.

Parts **a** and **b** of Figure 4 describe the structurally sensitive 1D WAXD patterns of pVBP(2,8). In order to eliminate thermal history, we collected the data of the first cooling and the subsequent, second heating. Upon the first cooling, as shown in Figure 4(a), the intensity of the low-angle peak/halo decreased, and the peak/halo became broader. And a reverse trend was observed during heating, as shown in Figure 4(b). Due to the lack of sharp change in either the intensity or the breadth of this low-angle peak/halo, it was difficult to judge from these two figures whether there were phase transitions during cooling and heating. Figure 4(c) shows the change in the *d*-spacing of the low-angle peak/halo with respect to temperature during the first cooling and the second heating for pVBP(2,8) on the basis of the results in parts a and b of

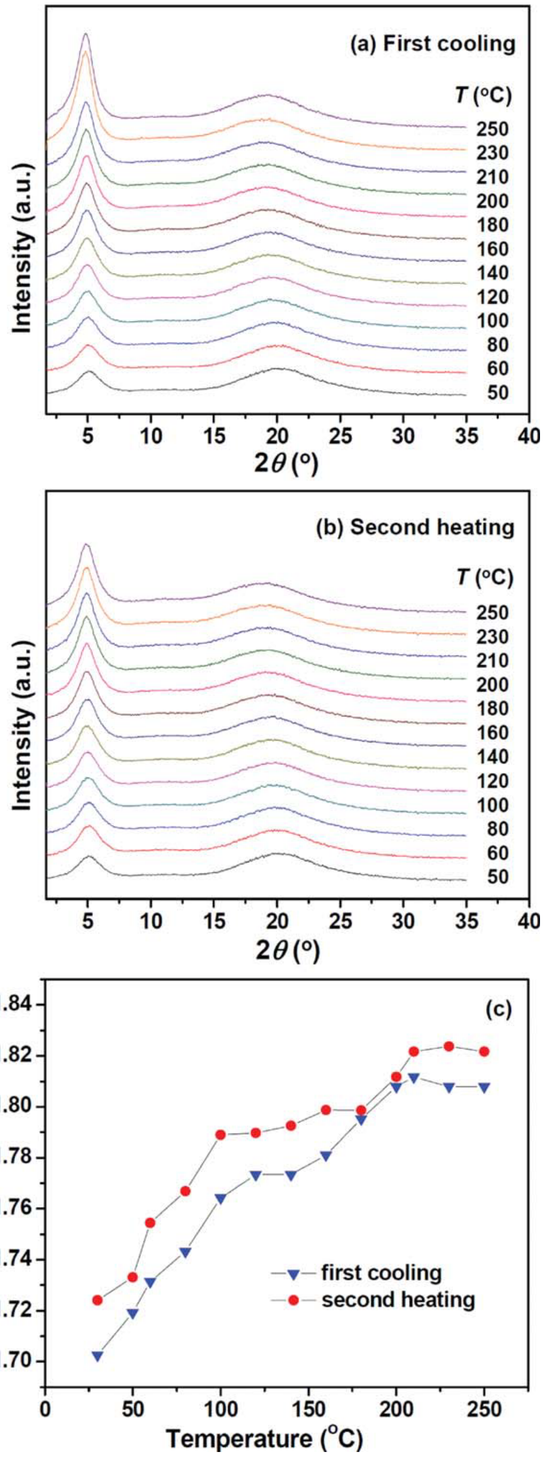

FIGURE 4 1D WAXD powder patterns of pVBP(2,8) during the first cooling (a) and the second heating (b) processes under a nitrogen atmosphere and the *d*-spacing of the low-angle peak/halo as a function of temperature (c) during the first cooling and the second heating as shown in (a) and (b). [Color figure can be viewed in the online issue, which is available at wileyonlinelibrary.com.]

Figure 4. For the first cooling curve, the first inflection at around 100 °C could be attributed to the glass transition, a second-order-like transition. The *d*-spacing remained almost unchanged until a sharp jump occurred at about 150 °C, followed by a plateau, which indicated a first-order transition. For the second heating curve, similar changes were also observed, although the jump at about 175 °C was less prominent than that in the first cooling curve, indicating an enantiotropic phase behavior of pVBP(2,8). Due to the lack of higher-order diffractions, the more ordered high-temperature phase could be a low-ordered LC phase. The structural characteristics (the jacketed structure and the simulated length, 2.10 nm, of the bulky side group being not far away from the *d*-spacing, 1.81 nm, of the low-angle peak at high temperatures) of the polymer and the schlieren-like texture shown in Figure 2(a) indicated that the LC phase was probably a Φ_N. Similar to the cases of typical MJLCPs, the low-angle peak corresponded to the columnar diameter, which was determined mainly by the length of the side-chain mesogen. Furthermore, because the LC phase formed at higher temperatures transformed into the amorphous phase during cooling, this polymer showed a re-entrant phase behavior, which could be due to entropic reasons, similar to some other MJLCPs reported previously.[9]

Because the 1D WAXD patterns lack dimensionality, we employed 2D WAXD to identify the phase structure of the sample pVBP(2,8). The sample was oriented by mechanical shearing at 160 °C during cooling from higher temperatures and annealed for a short time. Due to the enantiotropic nature of the LC phase, we conducted variable-temperature, 2D WAXD experiments. Parts a, b, and c of Figure 5 shows 2D WAXD patterns of the oriented, annealed sample at 200 °C through three orthogonal directions. The patterns in parts a and b of Figure 5 were virtually identical when the shearing direction was along the equatorial direction. A pair of sharp arcs could be observed in the low-angle region on the meridian, indicating the existence of ordered structures on the nanometer scale with lattice planes oriented primarily parallel to the equatorial direction. In addition, the scattering halo at a 2θ of about 20° in the high-angle region was more or less concentrated on the equator with rather broad azimuthal distributions, indicative of subnanometer structures with a short-range order existing mainly along the meridian direction. On the other hand, a sharp low-angle ring and a diffuse ring-like high-angle halo are shown in Figure 5(c) with the X-ray beam parallel to the shearing direction, demonstrating a rotational isotropy with the shear direction as the axis. These three patterns served as additional evidence to support that the high-temperature LC phase of pVBP(2,8) was a Φ_N.

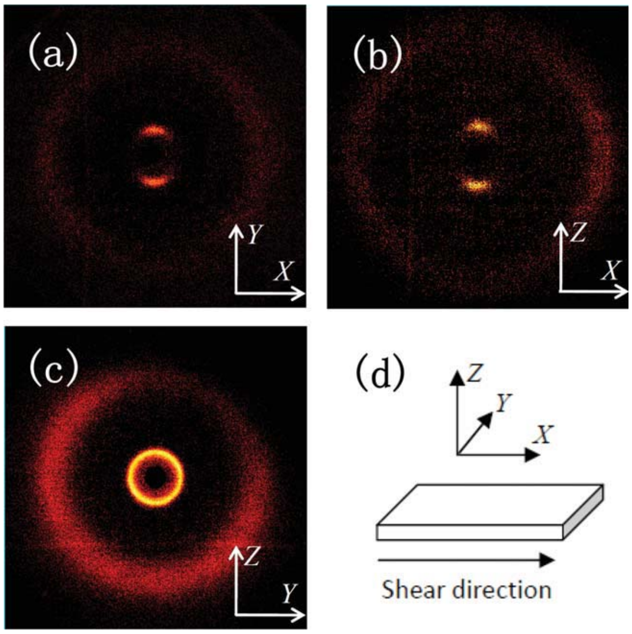

FIGURE 5 2D WAXD patterns of a sheared pVBP(2,8) sample recorded with the X-ray incident beam along *Z* (a), *Y* (b), and *X* (c) directions at 200 °C; the shearing geometry (d). [Color figure can be viewed in the online issue, which is available at wileyonlinelibrary.com.]

For the polymers pVBP(m,8) (m = 4, 6, 8, 10, 12), their 1D WAXD patterns were similar. With pVBP(8,8) as an example, parts a and b of Figure 6 show the 1D WAXD patterns of the sample during the first heating and the subsequent cooling. The isotropic sample prepared by solution-casting from a THF solution rendered an amorphous halo in the low-angle region at low temperatures. Upon the first heating, the intensity of the scattering halo increased slightly in Figure 6(a). When the temperature reached 160 °C which was much higher than the T_g of the polymer, a sharp diffraction peak at a 2θ of 4.72° (d = 1.87 nm) developed, indicating the existence of an ordered phase, possibly an LC phase. Combining with the PLM results, we could conclude that it was truly an LC phase. On the other hand, the scattering halo in the wide-angle region remained as a halo which moved to higher angles with increasing temperature due to thermal expansion. No higher-order diffractions of the low-angle peak could be observed in the 1D WAXD experiments, even when we attempted with more sample amounts or longer exposure times. Upon cooling, the sharp peak which originated from the LC phase disappeared at temperatures below 120 °C, and the low-angle scattering halo reappeared [Fig. 6(b)], which suggested that the ordered structure formed at high temperatures transformed into the low-temperature amorphous phase. Therefore, pVBP(8,8) also exhibited an enantiotropic, re-entrant phase behavior.

1D WAXD patterns of all the pVBP(m,8) polymers at 250 °C are presented in Figure 7 and the corresponding *d*-spacing values of the low-angle peak/halo are summarized in Table 2. Table 2 also lists the calculated lengths of the side groups of the polymers along with the temperatures at which the LC phases started to develop. As shown in Figure 7, only an amorphous halo could be observed in the high-angle region for all the polymers. In the low-angle region, the pattern of pVBP(1,8) showed a scattering halo. The pattern of pVBP(2,8) exhibited a relatively broad diffraction peak, and those of the other pVBP(m,8) (m = 4, 6, 8, 10, 12) samples

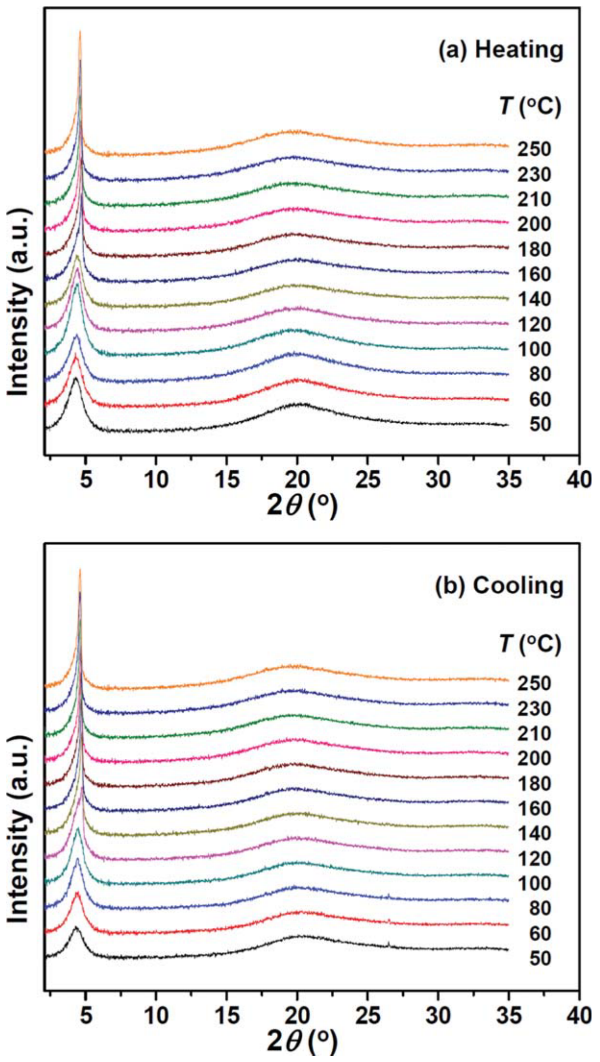

FIGURE 6 1D WAXD powder patterns of pVBP(8,8) during the first heating (a) and the first cooling (b) processes under a nitrogen atmosphere. [Color figure can be viewed in the online issue, which is available at wileyonlinelibrary.com.]

had a sharp diffraction peak, revealing the presence of ordered structures, possibly columnar phases for these jacketed polymers. The *d*-spacing values of the low-angle peak/halo for the polymers were comparable to the calculated lengths of the side chains under the assumption that the *n*-alkyl tails were in an all-*trans* conformation, indicating that the low-angle peak/halo was associated with the size of the side groups, which affected the phase structure. On the other hand, the *d*-spacing values were all smaller than the calculated side-chain lengths, indicating that the *n*-alkyl tails adopted a partially interdigitated packing. The more the difference between the experimental *d*-spacing value and the calculated side-group length for each polymer, the more degree of interdigitation. For the LC pVBP(m,8) (m = 2, 4, 6, 8, 10, 12), when m increased, this difference became larger, suggesting that the alkyl tails were packed in a more interdigitated manner with increasing m.

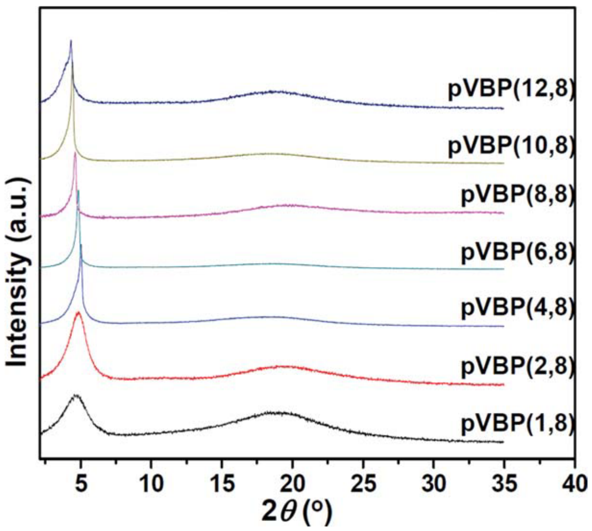

FIGURE 7 Set of 1D WAXD patterns of all the polymers recorded at 250 °C. [Color figure can be viewed in the online issue, which is available at wileyonlinelibrary.com.]

The phase transition temperatures, obtained from 1D WAXD measurement, of all the polymers are summarized in Table 2. They were strongly dependent on the difference in lengths of alkyls on the 4 and 4′ positions of biphenyl in the mesogen. For the pVBP(m,8) (m = 2, 4, 6, 8, 10, 12) polymers, the transition temperature was the lowest for pVBP(8,8), and, with the exception of pVBP(2,8), it generally increased with the increase or decrease of the alkyl ester tail, which indicated that the smaller the difference in the lengths of the terminal alkyl groups, the easier the formation of the liquid crystalline phase. The terminal alkyl groups in the mesogens of MJLCPs reported previously were the same, and this phenomenon has not been reported before.

Variable-temperature, 2D WAXD experiments were carried out to further identify the phase structures of pVBP(m,8) (m = 4, 6, 8, 10, 12) samples. These experiments demonstrated different 2D WAXD patterns, although the phase transition

TABLE 2 *d*-Spacing Values, Calculated Side-Group Lengths, and LC-Forming Temperatures of the pVBP(m,8) Polymers

Sample	*d* (nm)[a]	*L* (nm)[b]	T_{LC} (°C)[c]
pVBP(1,8)	1.86	1.96	–
pVBP(2,8)	1.81	2.10	180
pVBP(4,8)	1.75	2.22	250
pVBP(6,8)	1.83	2.36	180
pVBP(8,8)	1.92	2.52	160
pVBP(10,8)	2.00	2.66	200
pVBP(12,8)	2.05	2.82	210

[a] *d*-Spacing values at 250 °C obtained by 1D WAXD.

[b] Calculated length of the side groups from the ether end to the ester end with the alkyl chains in all-*trans* conformation.

[c] Temperature at which the LC phase was formed on the basis of 1D WAXD experiments.

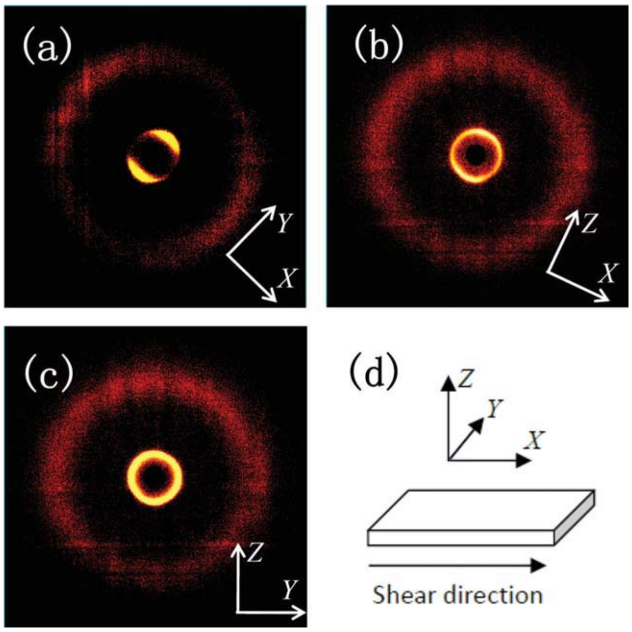

FIGURE 8 2D WAXD patterns of a sheared pVBP(6,8) sample recorded with the X-ray incident beam along *Z* (a), *Y* (b), and *X* (c) directions at 200 °C; the shearing geometry (d). [Color figure can be viewed in the online issue, which is available at wileyonlinelibrary.com.]

behaviors and textures of the aforementioned polymers from 1D WAXD and PLM experiments appeared to be similar.

A film sample of pVBP(6,8) was mechanically sheared at 145 °C and annealed for several hours. Parts a, b, and c of Figure 8 show the 2D WAXD patterns with the X-ray incident beam perpendicular (along *Y* or *Z* direction, with the *X* direction as the equatorial direction) and parallel (along *X* direction) to the shear direction at 200 °C. The similarity of these patterns to those in Figure 5 suggested that the pVBP(6,8) sample also developed a Φ_N phase at high temperatures. Similar patterns were also observed with other pVBP(m,8) (m = 4, 10, 12) polymers, indicative of Φ_N phases for these polymers.

In contrast, the 2D WAXD patterns (Fig. 9) of a pVBP(8,8) film sample mechanically sheared at 135 °C and annealed for several hours were different from those of pVBP(2,8) and pVBP(6,8); in particular, the difference was in the pattern obtained with the X-ray incident beam along the shear direction. Parts a and b of Figure 9 was similar to Figures 5(a,b) and 8(a,b). On the other hand, Figure 9c shows an interesting pattern. The low-angle diffraction exhibited an "X" pattern. The azimuthal scan of the low-angle diffraction arcs displayed four maxima which were separated by 90° from the adjacent ones [Fig. 9(d)], indicating a fourfold symmetry. There were no higher-order diffractions discernible in parts a, b, and c of Figure 9. Therefore, the pVBP(8,8) sample developed a columnar nematic phase with a local fourfold symmetry. Such a mesophase could be termed as a tetragonal columnar nematic (Φ_{TN}) phase, which, to the best of our knowledge, has not been reported before for MJLCPs. Comb-like LCPs from ionic complexation of dendronized polymers and lipids[41,42] have been reported to self-organize into tetragonal columnar mesophases, phases more ordered than Φ_{TN}, by tuning the generation and lipid chain length. Upon cooling, this Φ_{TN} phase disappeared, and the sample became amorphous, in agreement with the 1D WAXD results, which confirmed that pVBP(8,8) also exhibited a re-entrant phase behavior.

Dependence of the Phase Structure on the Difference of Alkyl-Tail Lengths

In this series of pVBP(m,8) polymers, two different types of LC phases and three types of phase transitions were observed, depending on the length of the terminal alkyl ester group, as shown in Figure 10. The polymer with the shortest methyl ester group was not liquid crystalline probably because the two ends on the side-chain biphenyl were so imbalanced that the polymer could not form a rod-like supramolecular mesogen. The longer alkyl tail in the ester side with increasing m increased the possibility of the formation of the supramolecular mesogen, and the pVBP(m,8) polymers could form liquid crystalline phases. They formed Φ_N phases when m was different from the number of carbon

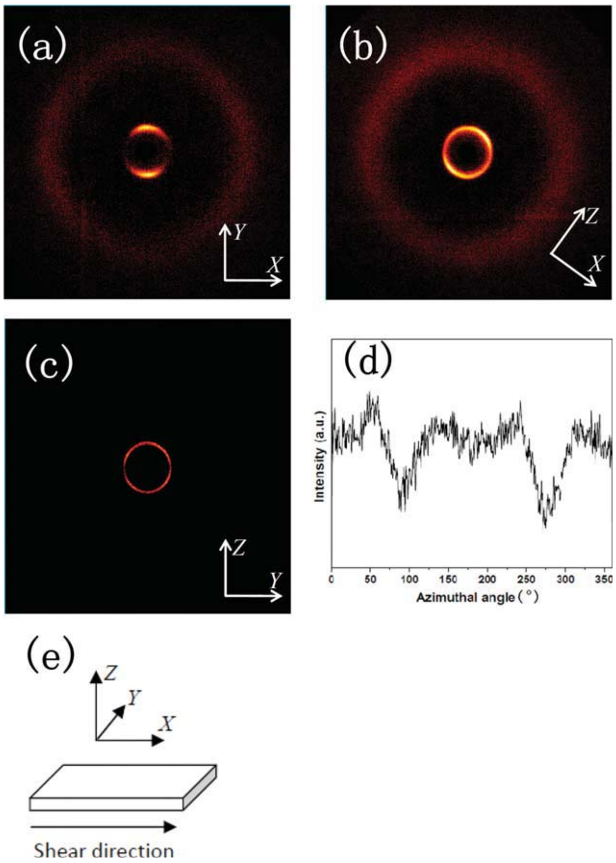

FIGURE 9 2D WAXD patterns of a sheared pVBP(8,8) sample recorded with the X-ray incident beam along *Z* (a), *Y* (b), and *X* (c) directions at 180 °C; azimuthal scan (d) of (c); shearing geometry (e). [Color figure can be viewed in the online issue, which is available at wileyonlinelibrary.com.]

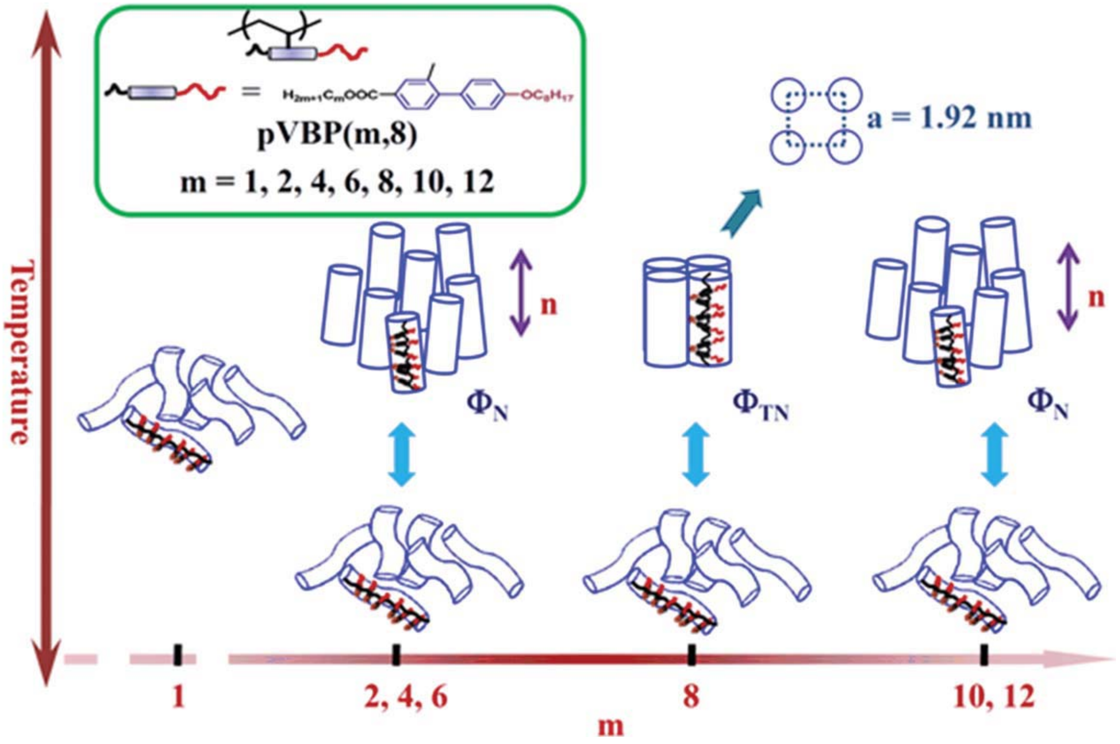

FIGURE 10 Schematic drawing of the thermotropic phase behavior of the polymers. [Color figure can be viewed in the online issue, which is available at wileyonlinelibrary.com.]

atoms in the alkyl ether tail (m = 2, 4, 6, 10, 12). The more symmetric sample pVBP(8,8) formed a more ordered liquid crystalline phase, Φ_{TN}, a columnar nematic phase with a local square lattice (a = 1.92 nm).

Optical Anisotropies of the Polymer Films

The polymers obtained in this work were easy to be processed into flexible freestanding films without the tendency of breaking or cracking (see Supporting Information, Fig. S2). The monomer precursor, mVBP(0,8), showed moderate Δn value of 0.2113, while the films of some of these polymers that we prepared possessed relatively high positive birefringence values (Table 3). The birefringence value was dependent on the length of the alkyl ester end group, but the trend was opposite to that in our previous report.[35] The discrepancy could be attributed to the fact that the birefringence value was mainly determined by the effective orientation of the rigid side chains. The improved orientation of the rigid side chains resulted in higher birefringence values with increasing m, although the underlying reason could not be determined. Our values were still lower than 0.02, a value regarded as viable for industrial applications, but by adjusting the length of terminal alkyl ester groups or by adding cyano or isothiocyanate functional groups to extend the length of the rigid side chain, we might obtain polymer films with higher birefringence values exceeding 0.02 without losing the excellent film-forming ability. Thus, we might utilize these films as optical compensation films. Related work is currently in progress.

TABLE 3 Refractive Indices and Birefringence Values of Some Polymer Films[a]

Polymer	Structure	$n_{//}$	$n_{\perp}$	Δn^{a}
pVBP(2,8)	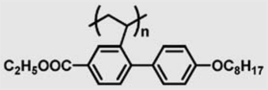	1.5613	1.5684	0.0071
pVBP(4,8)	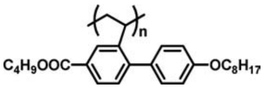	1.5523	1.5622	0.0099
pVBP(10,8)	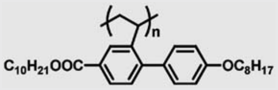	1.5368	1.5516	0.0148

[a] Measured according to the procedure described in literature.[39]

CONCLUSIONS

In summary, we successfully synthesized a novel series of MJLCPs of poly(alkyl 4′-(octyloxy)-2-vinylbiphenyl-4-carboxylate) pVBP(m,8) (m = 1, 2, 4, 6, 8, 10, 12), with biphenyl-based side chains containing alkyl groups of different lengths in the two ends of biphenyl via conventional free radical polymerization. All the polymers were thermally stable, and their T_g values decreased with increasing tail length due to increased internal plasticization. While pVBP(1,8) showed no liquid crystallinity, other pVBP(m,8) polymers (m = 2, 4, 6, 8, 10, 12) all exhibited columnar phases at high temperatures, and the LC phases transformed into the amorphous state upon cooling. The asymmetric substitution of the tails in the side-chain biphenyl affected the phase structures of these MJLCPs. The more symmetric polymer pVBP(8,8) developed a more ordered columnar phase (Φ_{TN}), while other LC pVBP(m,8) polymers formed Φ_N phases. Furthermore, the smaller the difference in the lengths of the alkyl tails in the side chains, the easier the formation of the LC phase. The polymers possessed good film-forming ability, and the films we tested had relatively high positive birefringence values, indicating their potential applications as optical compensation films in LCDs.

Financial support from the National Natural Science Foundation of China (Grant Nos.: 20634010, 20874002, 20974002, and 20990232) is gratefully acknowledged.

REFERENCES AND NOTES

1 Blumstein, A. Polymeric Liquid Crystals; Plenum Press: New York, 1985.

2 Finkelmann, H.; Wendorff, H. J. In Polymeric Liquid Crystals; Blumstein, A., Ed.; Plenum Press: New York, 1985; p 295.

3 Zhou, Q. F.; Li, H. M.; Feng, X. D. Macromolecules 1987, 20, 233–234.

4 Zhou, Q. F.; Zhu, X. L.; Wen, Z. Macromolecules 1989, 22, 491–493.

5 Wan, X. H.; Zhang, F.; Wu, P. Q.; Zhang, D.; Feng, X. D.; Zhou, Q. F. Macromol Symp 1995, 96, 207–218.

6 Xu, G. Z.; Wu, W.; Shen, D. Y.; Hou, J. N.; Zhang, S. F.; Xu, M.; Zhou, Q. F. Polymer 1993, 34, 1818–1822.

7 Ye, C.; Zhang, H. L.; Huang, Y.; Chen, E. Q.; Lu, Y.; Shen, D.; Wan, X. H.; Shen, Z.; Cheng, S. Z. D.; Zhou, Q. F. Macromolecules 2004, 37, 7188–7196.

8 Yin, X. Y.; Ye, C.; Ma, X.; Chen, E. Q.; Qi, X. Y.; Duan, X. F.; Wan, X. H.; Cheng, S. Z. D.; Zhou, Q. F. J Am Chem Soc 2003, 125, 6854–6855.

9 Zhao, Y. F.; Fan, X. H.; Wan, X. H.; Chen, X. F.; Yi, Y.; Wang, L. S.; Dong, X.; Zhou, Q. F. Macromolecules 2006, 39, 948–956.

10 Chai, C. P.; Zhu, X. Q.; Wang, P.; Ren, M. Q.; Chen, X. F.; Xu, Y. D.; Fan, X. H.; Ye, C.; Chen, E. Q.; Zhou, Q. F. Macromolecules 2007, 40, 9361–9370.

11 Chen, S.; Zhang, L. Y.; Gao, L. C.; Chen, X. F.; Fan, X. H.; Shen, Z.; Zhou, Q. F. J Polym Sci Part A: Polym Chem 2009, 47, 505–514.

12 Zhu, Z. G.; Zhi, J. G.; Liu, A. H.; Cui, J. X.; Tang, H.; Qiao, W. Q.; Wan, X. H.; Zhou, Q. F. J Polym Sci Part A: Polym Chem 2007, 45, 830–847.

13 Yu, Z. N.; Tu, H. L.; Wan, X. H.; Chen, X. F.; Zhou, Q. F. J Polym Sci Part A: Polym Chem 2003, 41, 1454–1464.

14 Degivenchy, E. T.; Guittard, F.; Bracon, F.; Cambon, A. Liq Cryst 1999, 26, 1163–1170.

15 Okamoto, H.; Okamoto, T.; Takenaka, S. Chem Lett 2000, 9, 1040–1041.

16 Sybo, B.; Bradley, P.; Grubb, A.; Miller, S.; Proctor, K. J. W.; Clowes, L.; Lawrie, M. R.; Sampson, P.; Seed, A. J. J Mater Chem 2007, 17, 3406–3411.

17 Fernandez-Blazquez, J. P.; Bello, A.; Perez, E. Macromolecules 2007, 40, 703–709.

18 Auad, M. L.; Kempe, M. D.; Kornfield, J. A.; Rendon, S.; Burghardt, W. R.; Yoon, K. Macromolecules 2005, 38, 6946–6953.

19 Gopinadhan, M.; Majewski, P. W.; Osuji, C. O. Macromolecules 2010, 43, 3286–3293.

20 Lee, K. M.; Han, C. D. Macromolecules 2002, 35, 6263–6273.

21 Nieuwhof, R. P.; Koudijs, A.; Marcelis, A. T. M.; Sudholter, E. J. R. Macromolecules 1999, 32, 6499–6506.

22 Omenat, A.; Hikmet, R. A. M.; Lub, J.; Sluis, P. V. Macromolecules 1996, 29, 6730–6736.

23 Tork, A.; Bazuin, C. G. Macromolecules 2001, 34, 7699–7706.

24 Xie, H. L.; Jie, C. K.; Yu, Z. Q.; Liu, X. B.; Zhang, H. L.; Shen, Z. H.; Chen, E. Q.; Zhou, Q. F. J Am Chem Soc 2010, 132, 8071–8080.

25 Percec, V.; Asandei, A. D.; Hill, D. H.; Crawford, D. Macromolecules 1999, 32, 2597–2604.

26 Percec, V.; Rudick, J. G.; Peterca, M.; Heiney, P. A. J Am Chem Soc 2008, 130, 7503–7508.

27 Rudick, J. G.; Percec, V. Acc Chem Res 2008, 41, 1641–1652.

28 Arumugam, S.; Vutukuri, D. R.; Thayumanavan, S.; Ramamurthy, V. J Am Chem Soc 2005, 127, 13200–13206.

29 Basu, S.; Vutukuri, D. R.; Shyamroy, S.; Sandanaraj, B. S.; Thayumanavan, S. J Am Chem Soc 2004, 126, 9890–9891.

30 Cheng, S. Z. D.; Li, F. M.; Savitski, E. P.; Harris, F. W. Trends Polym Sci 1997, 5, 51–58.

31 Kuo, C. L.; Miyashita, T.; Suzuki, M.; Uchida, T. Appl Phys Lett 1996, 68, 1461–1463.

32 Lee, S.; Khosravani, R.; Peng, J.; Grubsky, V.; Starodubov, D. S.; Willner, A. E.; Feinberg, J. IEEE Photon Technol Lett 1999, 11, 1277–1279.

33 Yoshiara, K.; Matsumoto, S.; Takabayashi, M.; Shimakura, Y.; Sugihara, T. Rev Laser Eng 2005, 33, 433–437.

34 Fukunaga, A.; Sato, Y.; Shimoda, K. Jpn Patent, JP 2009025789–A, 2009.

35 Chen, S.; Zhang, L. Y.; Guan, X. L.; Fan, X. H.; Shen, Z.; Chen, X. F.; Zhou, Q. F. Polym Chem 2010, 1, 430–433.

36 Brandsma, L.; Vasilevsky, S. F.; Verkruijsse, H. D. Application of Transition Metal Catalysts in Organic Synthesis; Springer: Berlin, 1999.

37 Zhang, L. Y.; Chen, S.; Zhao, H.; Shen, Z. H.; Chen, X. F.; Fan, X. H.; Zhou, Q. F. Macromolecules 2010, 43, 6024–6032.

38 Guan, X. L.; Zhang, L. Y.; Zhang, Z. L.; Shen, Z. H.; Chen, X. F.; Fan, X. H.; Zhou, Q. F. Tetrahedron 2009, 65, 3728–3732.

39 Harris, F. W.; Zhang, D.; Zheng, X. L.; Germroth, T. C.; Kuo, T.; Jing, J. K.; King, B. M. Int. Patent, WO 2008121583–A1, 2008.

40 Chen, S.; Jin, Y.; Hu, S.; Hu, M. Polym Commun 1987, 28, 208–211.

41 Canilho, N.; Kasemi, E.; Mezzenga, R.; Schluter, A. D. J Am Chem Soc 2006, 128, 13998–13999.

42 Canilho, N.; Kasmi, E.; Schluter, A. D.; Mezzenga, R. Macromolecules 2007, 40, 2822–2830.